Ionics (2024) 30:1627–1638
https://doi.org/10.1007/s11581-024-05373-z

RESEARCH

Preparation of electrospun polyacrylonıtrile (PAN) nanofıber membrane gel electrolyte and its application in TiO_2-based electrochromic devices

H. N. M. Sarangika[1] · G. K. R. Senadeera[2,3] · M. A. K. L. Dissanayake[3]

Received: 19 August 2023 / Revised: 13 December 2023 / Accepted: 3 January 2024 / Published online: 6 January 2024

Abstract
Electrochromic devices based on nanofiber membrane gel electrolytes offer several advantages over polymer gel electrolytes. Many advantages, such as high chemical stability, easy handling, less leakage, a wide working temperature range, and a long cycle life, show high compatibility of nanofiber membrane electrolytes in different electrochemical power devices. In this work, we have succeeded in replacing the liquid electrolyte with a nanofiber membrane–based gel electrolyte prepared by the electrospinning method and applied in electrochromic devices (ECD). Polyacrilonitrile (PAN)–based nanofibers were deposited on a spin-coated SnO_2 layer, prepared on a fluorine-doped tin oxide (FTO) glass substrate. The thickness of the fiber mat was varied by changing the time of the electrospinning. Gel-type membrane electrolyte was prepared by soaking the nanofiber membrane electrode in the 1 M $LiClO_4$ in propylene corbonate (PC) solution. TiO_2 electrochromic electrode was prepared by the "doctor blade" method. ECDs were fabricated with the configuration of FTO glass/TiO_2/PAN-based nanofiber membrane gel polymer electrolyte/SnO_2/FTO glass by sandwiching the two electrodes. Electrochromic performance of ECDs fabricated with nanofiber membrane gel electrolyte was compared with ECDs fabricated with liquid electrolyte (1 M $LiClO_4$ in PC) and PAN-based conventional gel electrolyte (PC (0.4 g) + ethylene carbonate (EC) (0.4 g) + $LiClO_4$ (0.03 g) + PAN). ECDs with nanofiber membrane gel electrolytes demonstrate a transmittance variation of 33.40% in the visible region which is 93% of the corresponding value obtained with liquid electrolyte–based ECD, whereas identical ECDs made with conventional gel electrolytes demonstrate a lower transmittance variation of 4.22%.

Keywords Electrospun nanofiber membrane · Gel electrolytes · Electrochromic devices · Electrospinning

Introduction

Electrochromism is the phenomenon that changes transmittance or reflectance of some materials reversibly when an appropriate current or potential is applied to it [1]. Applying electric current or potential leads to the reduction of electrochromic material (EC), and it causes the generation of different visible region electronic absorption bands. Transition metal oxides such as WO_3 and TiO_2 change their transmission under the influence of an electrical current or potential. The change of transmittance is due to the color change of the EC material. The color change of electrochromic material is usually between a transparent (bleaching) state and a colored state or between two colored states. Coloring or bleaching of the EC material is a consequence of the insertion or extraction of electrons or metal ions in/from the EC material. This interesting behavior of the electrochromic material can be used to prepare electrochromic devices (ECD) for controlling the flow of light and heat that pass through the windows of building and vehicles, rearview mirrors, etc. [2–4].

ECD is composed of three components; a working electrode (EC electrode), an ion transportation medium (electrolyte), and a counter electrode. They are arranged in a layered configuration in which a working electrode and a counter electrode (CE) are physically separated by ion-conducting liquid, quasi-solid (gel), or solid electrolyte. When the ECD

✉ H. N. M. Sarangika
sarangikah@appsc.sab.ac.lk

[1] Department of Physical Science and Technology, Sabaragamuwa University of Sri Lanka, Belihuloya, Sri Lanka

[2] Department of Physics, The Open University of Sri Lanka, Nawala, Nugegoda, Sri Lanka

[3] National Institute of Fundamental Studies, Kandy, Sri Lanka

is subjected to an electric field, it undergoes reversible color change according to the insertion or extraction of metal ions or electrons. ECDs have been investigated for years for potential commercial applications. However one of the major problems associated with the commercialization of electrochromic devices is their cost. Most of the ECDs used transition metal oxides such as WO_3 as the electrochromic material and CeO_2 as the counter electrode which are very expensive compared with other metal oxides [4].

Although ECDs fabricated with liquid electrolytes show high performances, many drawbacks limit the practical application of ECDs. In most cases, lithium perchlorate in propylene carbonate was used as the solution electrolyte. The leakage of electrolyte solution, weight gain from the solution, and low chemical stability of liquids are the main drawbacks of these display devices [1, 5, 6]. To overcome these problems, many research investigations have been devoted to the development of ECDs employing solid or quasi-solid polymer electrolytes (QSPEs). Solid polymer electrolytes based on poly (ethylene oxide) (PEO), polyvinyl butyral (PVB), polyacrylonitrile (PAN), polymethyl methacrylate (PMMA), and inorganic ion conductors have been investigated [7–10]. Although solid polymer electrolytes solve some drawbacks, the performances of ECDs with these electrolytes have been rather low in making practical devices. This is because of the low ionic conductivity (10^{-9} to 10^{-5} S cm^{-1}) of the solid polymer electrolyte at room temperature.

On the other hand, quasi-solid polymer or gel electrolytes have emerged as a promising solution to address challenges in many of the electrochemical devices such as solar cells, and energy-storing devices like Li ion batteries. QSPEs offer a unique combination of solid-like mechanical properties and ionic conductivity, stemming from the incorporation of a polymer matrix that immobilizes liquid electrolytes.

Another alternative method to replace these liquid electrolytes is to use polymer nanofibers. Various methods are employed in the production of nanofibers, encompassing techniques such as electrospinning, melt-spinning [11], molecular assembly [12], and chemical vapor deposition [13]. Among these methods, electrospinning emerges as highly advantageous and convenient for crafting a diverse array of organic and/or inorganic nanofibers under ambient conditions of temperature and pressure. Electrospun nanofibers offer a range of advantages attributed to their unique characteristics [14]. The high surface area-to-volume ratio of these ultrafine fibers, which are created by electrospinning, gives them exceptional mechanical strength and flexibility. Their fine scale and high porosity make them excellent candidates for applications in filtration, drug delivery, and tissue engineering. The tunable properties of electrospun nanofibers, achieved through precise control of fabrication parameters, allow for customization to meet specific requirements in electronics, sensors, and catalysis. Moreover, their lightweight yet robust nature makes them suitable for diverse industries, highlighting their potential to revolutionize various technological applications [15–17]. This technique involves applying an electric field to a polymer solution or melt, resulting in the extrusion of ultrafine fibers [14, 18, 19]. These nanofibers possess a high surface area-to-volume ratio and tunable properties, making them attractive for various applications in fields such as materials science, biomedical engineering, and energy storage. The dimensions and structure of the electrospun nanofibers can be finely tuned by adjusting various electrospinning parameters, encompassing applied voltage, flow rate, viscosity, and electrical conductivity of the polymer solution, as well as the temperature and humidity within the apparatus [18–22].

In the electrospinning technique, a variant of the electrostatic spraying is used. By applying a high voltage, a liquid jet is formed as an electrified jet and it is continuously stretched due to the electrostatic repulsion between the surface charges and the evaporation of the solvent process leading to the formation of a long and thin thread having a diameter of tens of nanometers. Properties of the nanofibers such as diameter, morphology, strength, pore size, and fiber thickness can be controlled by applying different starting parameters to the electrospinning process. High porous fiber membrane is essential for filling liquid electrolytes without restricting ionic mobility and diffusion nanofiber [23, 24].

Various types of ECDs, such as flexible, foldable, stretchable, and wearable, have recently been tested. It has also been reported that electrochromism and energy storage effectiveness can be combined into a single device. Such dual-function ECDs can adjust the sunlight and solar heat inside the building and at the same time can be used as energy storage devices [15, 25, 26]. Apart from that, stretchable and wearable electrochromic devices are tested for application in future smart clothes [27]. Along with the above successes, some challenges still remain to be tackled in electrochromic devices. Suitable electrolyte systems that enable robust cycling and fast switching are also needed. Therefore, significant efforts are required to develop high-performance electrochromic devices and integrate them into multifunctional systems.

Therefore, considering all above factors, we have explored the possibilities of using low-cost materials in these devices while, at the same time, replacing the liquid electrolytes with nanofiber membrane–based quasi-solid-state (gel) electrolytes. The main objective of this research is to find the performance of the nanoparticulate TiO_2 film as an electrochromic material and low-cost SnO_2 as the counter electrode together with polyacrylonitrile (PAN)–based nanofiber membrane gel polymer electrolyte in ECDs.

Materials and methods

Materials

Polyacryconitrile (PAN, Avg. Mw 150,000) was purchased from Sigma-Aldrich and N,N-dimethylformamide (DMF), propylene carbonate (PC), and lithium perchlorate ($LiClO_4$) with purity > 98% were purchased from Fluka. Fluorine-doped SnO_2-layered (FTO) glass (sheet resistance 12 Ω/cm^2) and commercially available titania (TiO_2) paste were purchased from Solaronix SA. SnO_2 colloidal solution (2.5 wt%, viscosity 3.5 cp) was purchased from Sigma-Aldrich.

Fabrication of TiO_2 electrochromic electrodes

According to Nihan et al., the interface between the TiO_2 mesoporous layer and the FTO substrate has a sizable resistance for ion transfer and storage [28]. By introducing a compact layer of much smaller TiO_2 particles, in between the FTO and the mesoporous TiO_2 layer, the interfacial resistance can be reduced so that the ion transfer and storage of the EC device can be facilitated. On the other hand, the thickness of the mesoporous layer is also effective for coloration efficiency [28]. In this work, it was observed that the thickness of the TiO_2 mesoporous layer could not be increased to achieve the best device performance due to the poor adhesion to the FTO substrate. This problem was overcome by introducing a compact TiO_2 layer in between the FTO substrate and the mesoporous TiO_2 layer.

At first, a compact layer of nanocrystalline TiO_2 films was prepared by spin coating on the pre-cleaned fluorine-doped conducting tin oxide (FTO) glass plates (active area 1.4 cm × 2.1 cm) using the solution prepared as follows: 5 ml of propon-1-Ol, 5 ml of acetic acid, 5 ml of tetra isopropyl orthotitanate (Fluka), 30 ml of ethanol, and one drop of nitric acid were mixed while keeping in an ice bath and stirred for 30 min. Then, one drop of the solution was placed on the pre-cleaned FTO glass plate and speaded on FTO by spin coating method (3000 rpm) [29]. The films were then put into the oven and calcined at 450 °C for 45 min. The thickness of the compact TiO_2 layer was measured by Veeco, Dektack 3 profilometer and the thickness was around 100 nm. Mesoporous nanocrystalline TiO_2 films were prepared on top of the above electrodes by coating a TiO_2 paste purchased from Solaronix Switzerland (Solaronix T) using the "doctor blade" method. Films were then sintered at 450 °C for 45 min. The thickness of the mesoporous TiO_2 layer was measured using a Veeco, Dektack 3 profilometer and thickness was found to be around 6.5 µm [30].

Preparation of SnO_2 counter electrode

Spin coating technique (5000 rpm) was used to prepare the SnO_2-based counter electrode on top of the FTO. A SnO_2-dispersed solution was used in the spinning solution and the films were prepared by spinning for 1 min. Then, the SnO_2-deposited films were calcined at 550 °C for 30 min. Thickness of the SnO_2 counter electrode layer was measured by using a SEM and the value was found to be 13.5 µm [31].

Preparation of the electrospinning solution and PAN nanofiber membranes

PAN nanofiber membranes were prepared by using a NABOND electrospinning system (NaBond Technologies, Hong Kong). First, different amounts of PAN were dissolved in a constant volume of DMF and the mixture was kept at 140 °C under stirring. Based on the viscosity of the PAN in the DMF solution, 11wt% PAN in DMF was selected for the electrospinning as this was the optimized PAN concetration to get the best nanofibers. Solutions with higher PAN concentration, due to their higher viscosity, could not pass smoothly through the syringe of the electrospinning equipment. The electrospinning was carried out for the optimized solution under different electrospinning parameters. The SEM images of the nanofiber mats were taken under the optimized conditions. At the most optimum stage, it was observed that the DC voltage between the spinner and the drum collector should be equal to 8 kVdc. A series of nanofibers was prepared at this optimized DC voltage but changing the flow rate. The flow rate of the polymer solution was optimized as 2 ml/h and the optimized drum speed was 270 rpm. Since the distance between the tip and the collector is strictly influenced by the morphology of the fiber, it was kept at 6.5 cm throughout the process. A schematic diagram of the electrospinning process with its optimized parameters is shown in Fig. 1. Prepared SnO_2-coated FTO glass substrates were attached to the aluminum foil keeping 1.4 cm × 2.1 cm space in the middle of the substrate. The drum collector was then covered by this aluminum foil using magic tapes so that the electrospun PAN nanofibers were deposited onto grounded, SnO_2-coated FTO plates [32]. Electrospun PAN nanofibers were prepared by applying the above-mentioned optimized parameters. Nanofiber membrane thickness was controlled by varying the spinning time from 5 to 25 min.

Electrolyte preparation

1 M $LiClO_4$ in PC was prepared and used as a liquid electrolyte. Conventional PAN-based gel electrolyte was prepared using the following receipe. 0.03 g of $LiClO_4$ was dissolved in 0.4 g of PC and 0.4 g of EC mixture under stirring few

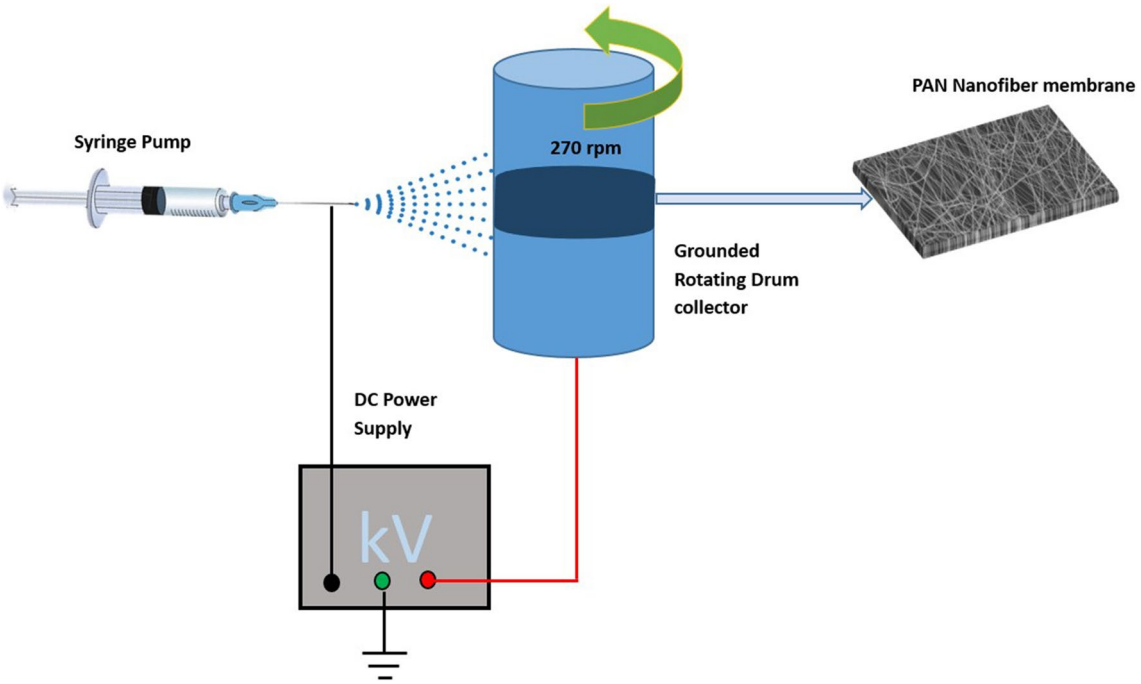

Fig. 1 Schematic diagram of the electrospinning process

minutes for complete dissolution. Then, 0.1 g of PAN was added to this solution [33]. The PAN-based nanofiber membrane gel electrolyte was prepared by adding 1 M $LiClO_4$ in PC dropwise onto the nanofiber mat deposited on the SnO_2-coated FTO glass plate.

Electrochromic cell assembly

TiO_2-coated FTO electrode was used as the working electrode and PAN nanofiber deposited SnO_2 substrate was used as the counter electrode. Three drops of 1 M $LiClO_4$ in PC were added to the membranes to form "gel" type nanofiber membrane electrolytes on SnO_2-coated electrode. ECDs having the configuration FTO/TiO_2/nanofiber membrane electrolyte/SnO_2/FTO were assembled as shown in Fig. 2.

Measurements

To check the structure of the nanofiber membrane, scanning electron microscopy (SEM; JEOL JSM-651LV) was used. The performance of the fabricated ECDs was checked and the transmittance variation with applied voltage was

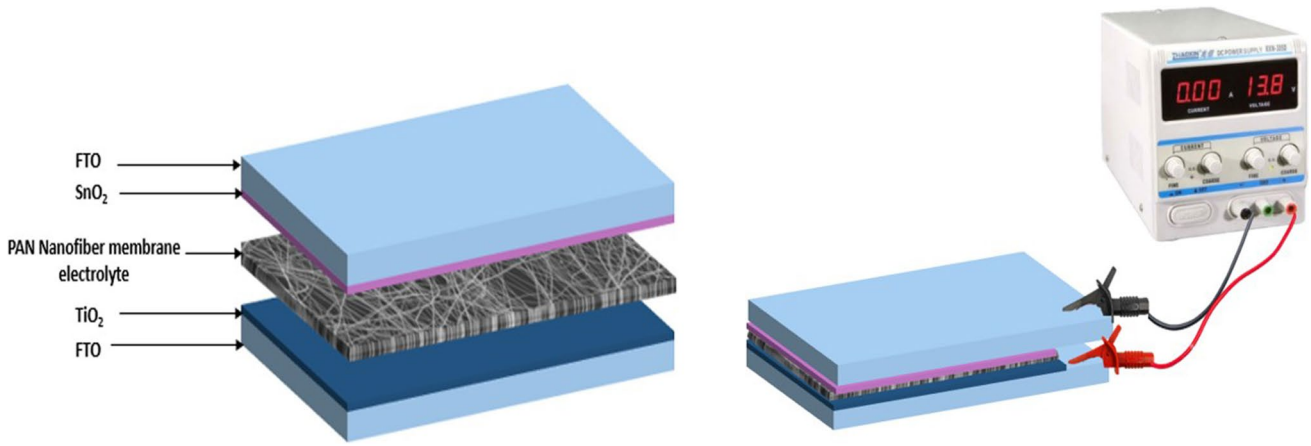

Fig. 2 Schematic diagram of ECDs having the configuration FTO/TiO_2/nanofiber membrane electrolyte/SnO_2/FTO

recorded using UV–visible optical spectra in the full wavelength range (190 nm and 1100 nm). The Shimadzu 2600 spectrophotometer was used to measure the transmittance vs. wavelength at different applied voltages. Cyclic voltammery was carried out using Metrohm Autolab (PGSTAT 128 N).

Results and discussion

Electrochromic electrode and counter electrode

Figure 3 shows the photographs of prepared transparent TiO_2 active electrode and SnO_2 counter electrode. Optical transmittance spectra of these electrodes confirmed relatively high transmittance (> 90) as shown in the figure.

Cyclic voltammetry studies were carried out to characterize the electrochemical properties of the TiO_2 thin film as the EC material. Electrochemical insertion and extraction were analyzed using a solution of 1 M $LiClO_4$ in PC as the electrolyte with the platinum and the standard calomel electrode (SCE) as the counter electrode and reference electrode respectively. Figure 4 shows cyclic voltammetry trace of the TiO_2 film coated on FTO by the "doctor blade" method. According to Fig. 4, no cathodic peaks are observed in the sample while a well-defined anodic peak is observed. The coloration of TiO_2 is a consequence of the simultaneous insertion of electrons and Li ions into the TiO_2 film, leading to the reduction of Ti^{+4} to Ti^{+3}. On electrochemical reduction, Ti^{+3} sites are generated to give the electrochromic effect turning its color to blue[7].

PAN nanofiber membrane

SEM pictures of the fabricated nanofibers were taken and Fig. 5 shows the top and cross-sectional view of the fiber membrane. Average diameter of the nanofiber is estimated and it is 1.2 µm (Fig. 5b). This value is comparable with

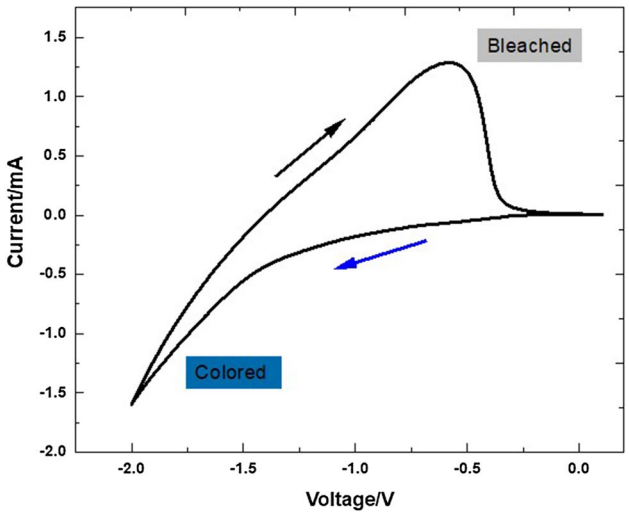

Fig. 4 Electrochemical study of TiO_2/FTO in 1 M $LiClO_4$ in PC (scan rate 10 $mVs.^{-1}$)

the average diameters of the polypyrrole nanofibers used to fabricate ECDs with WO_3 by Dulgerbaki et al. [34]. It can be seen that fibers have a three-dimensional structure and a large number of pores that lead to the uptake of a large amount of electrolyte solution.

As can be seen in Fig. 5d, several cross-linking points on the membrane directly affect the strength of the fiber mat [35, 36]. The exact value of the thickness of the fiber membrane can not be measured. Figure 5c shows the cross-sectional view of the fiber mat prepared with 10-min spinning time and according to that the thickness of the fiber mat is around 34 µm.

We believe that the PAN nanofibers play an inert role to trap and hold the solution electrolyte "1 M $LiClO_4$ in PC" and give it a "gel" behavior. Among the polymer hosts studied so far, the PAN-based electrolytes offer a homogenous, hybrid electrolyte film in which the salt and the plasticizer

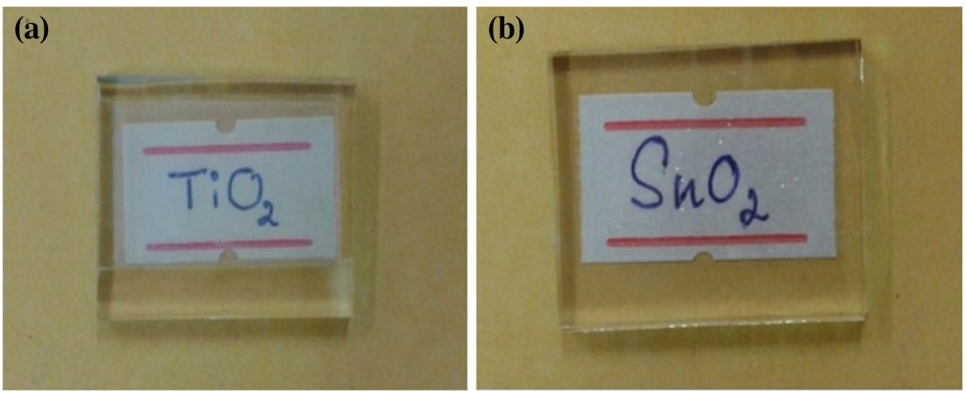

Fig. 3 **a** Transparent TiO_2 working electrode. **b** SnO_2 counter electrode

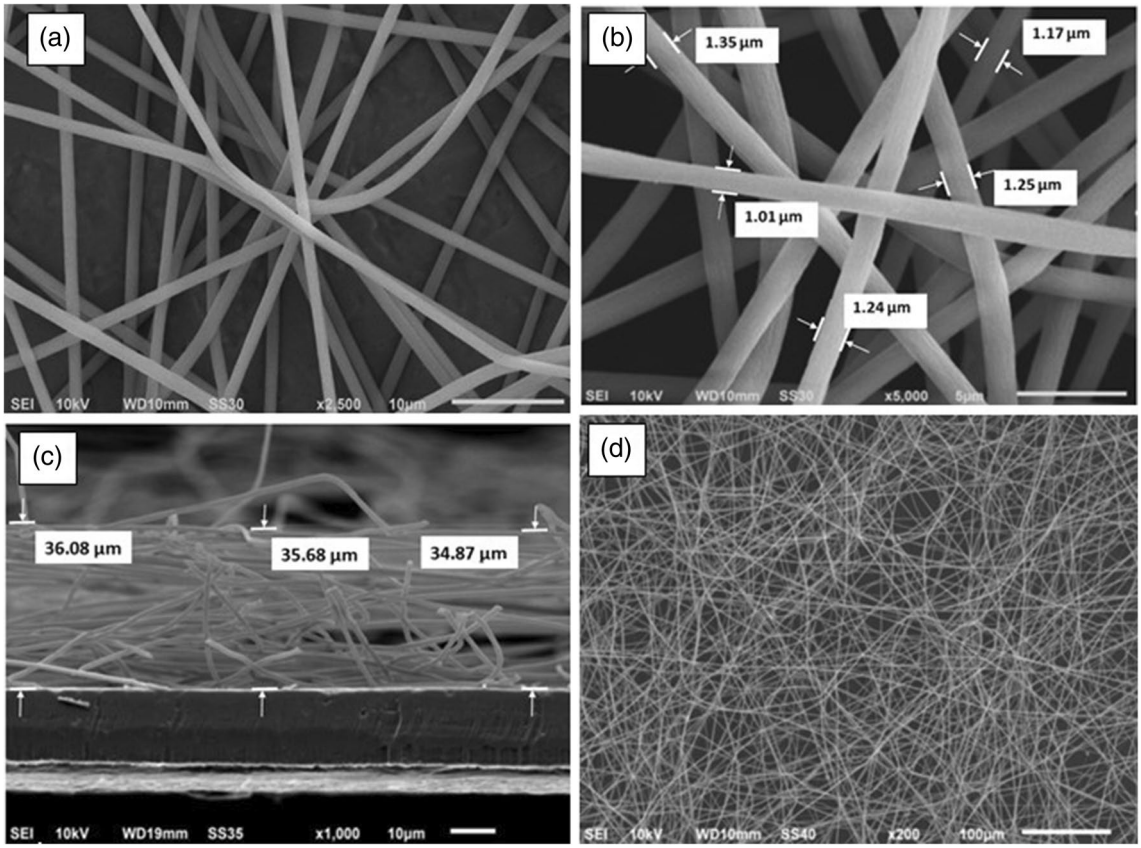

Fig. 5 SEM images of the **a** PAN nanofiber membrane produced by the electrospinning, **b** top view of the membrane different magnification, **c** cross-sectional view of the fiber membrane, and **d** top view of the nanofiber mat

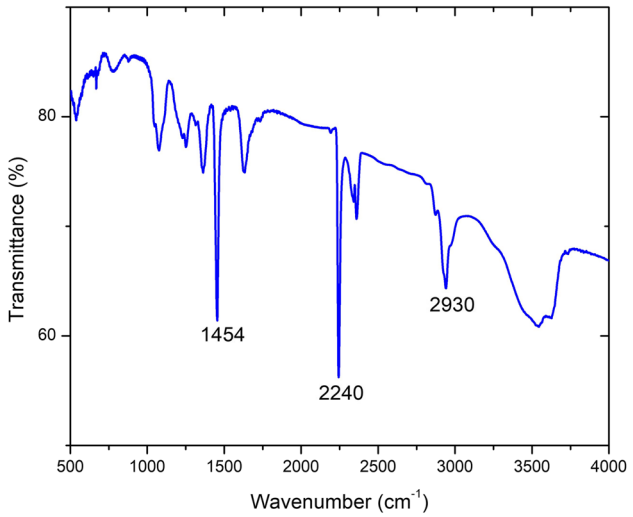

Fig. 6 FTIR spectra of pristine PAN nanofibers

were molecularly dispersed. The FTIR spectra of PAN are presented in Fig. 6. Pure PAN nanofibers displayed the characteristic absorption peaks of nitrile ($-C \equiv N$) group at around 2240 cm^{-1}. Also methylene (CH_2) group of PAN showed characteristic bands in the regions 1454 cm^{-1} and 2930 cm^{-1} [37].

Electrochromic device performance

In the first part of this study, thickness optimization of the nanofiber membrane electrolyte was done by varying the spinning time. Figure 7 shows the transmittance spectra of the ECD with different nanofiber membrane thicknesses. According to Fig. 7, the highest optical contrast was obtained for the 10-min electrospun nanofiber membrane electrolyte. Further increase of the electrospinning time increases the film thickness of the fiber mat and positively affects for up taking more liquid electrolyte. However, the higher thickness of the fiber mat is caused to reduce the initial transmittance at bleached state. Therefore, the optimized time for electrospinning is 10 min.

Table 1 summarizes the transmittance difference of the fabricated ECDs of configuration FTO/TiO_2/nanofiber membrane polymer electrolyte (PAN)/SnO_2/FTO with spinning time which controls the film thickness. To change the electrochemical states of the EC device, different voltages were applied across the two electrodes and a color change

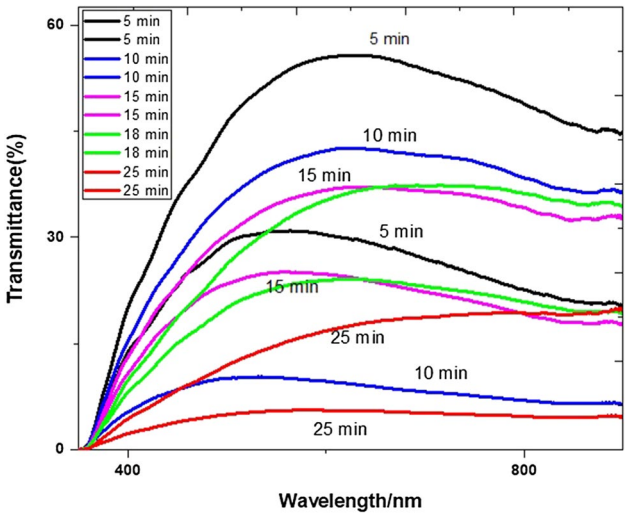

Fig. 7 Optimization of the nanofiber membrane thickness with optical transmittance spectra

Table 1 Transmittance variation of the ECDs at their bleached state and colored state with different thicknesses of the nanofiber membrane electrolyte

Sample No	Spinning time/min	Transmittance at 4.2 V	Transmittance at 0 V	ΔT
1	05	29.63	55.74	26.11
2	10	13.09	46.49	33.4
3	15	11.49	38.78	27.29
4	20	15.01	33.76	18.75
5	22	16.67	27.64	10.97

between dark blue and bleached was observed. The transmittance of the ECD was varied depending on the voltage applied across the device. The bleached or colorless state of the device was observed when applying an appropriate negative voltage (0.2 V) across the two electrodes. It confirms the reversible ion insertion and extraction process of the ECD when switching between positive and negative potentials. Pictures of the corresponding electrochemical states of the EC device are shown in Fig. 8. ECD at its intermediate state (voltage applied = 2.0 V) and fully colored state (voltage applied = 4.0 V) is shown in Fig. 8.

According to Table 1, maximum transmittance variation was observed for the electrospun membrane electrolyte soaked with the 1 M $LiClO_4$ in PC liquid electrolyte having 10-min spinning time. Initial transmittance at their bleached state has reduced with the increase of the spinning time. An increase in fiber membrane thickness reduces the light that can be transmitted. At the colored state, a thin electrospun membrane electrolyte shows a high transmittance value as compared with a thick electrospun membrane electrolyte. When the thickness of the fiber membrane is low, the number of cross-linking points becomes less while the pore sizes inside the fiber membrane become high. This is the cause for the up taking less amount of liquid electrolyte by the polymer membrane [32]. The less amount of liquid electrolyte retained in the polymer membrane reduces the number of mobile Li ions that are used to color the TiO_2 film. When the spinning time increases, the thickness of the membrane and the no of cross-linking points will increase while decreasing the pore sizes. Therefore, the membrane can uptake large amounts of electrolyte solution and this will facilitate to increase in the number of Li ions that intercalate into TiO_2 film. Further increase in membrane thickness limits the mobility of Li ions inside the membrane with a high concentration of the polymer in the membrane. This blocking effect again reduces the number of Li ions intercalating into the electrochromic film. From Table 1, it can be seen that the best chromatic contrast (ΔT) given by Eq. 1 is for 10 min of spinning time.

$$\text{Chromatic contrast}(\Delta T) = T_b(\lambda) - T_c(\lambda) \quad (1)$$

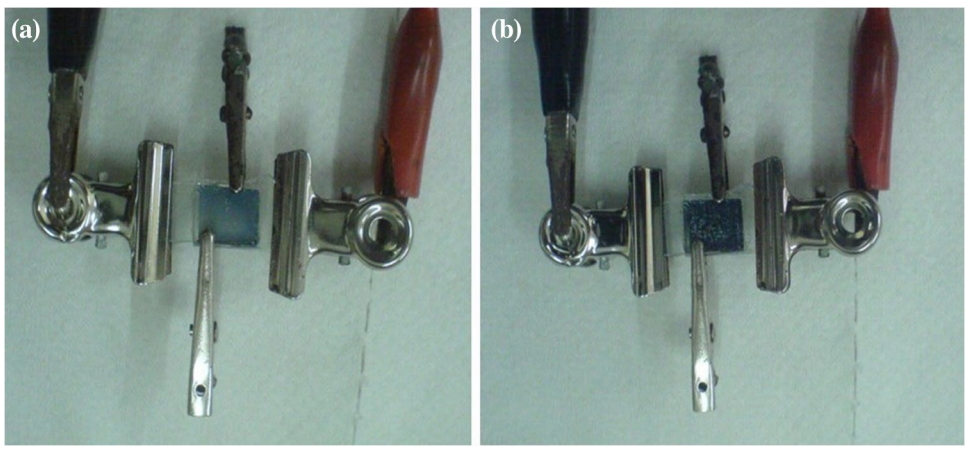

Fig. 8 Photographs of the ECD of the configuration FTO/TiO_2/PAN-based nanofiber membrane gel polymer electrolyte/SnO_2/FTO at **a** partially colored and **b** fully colored state

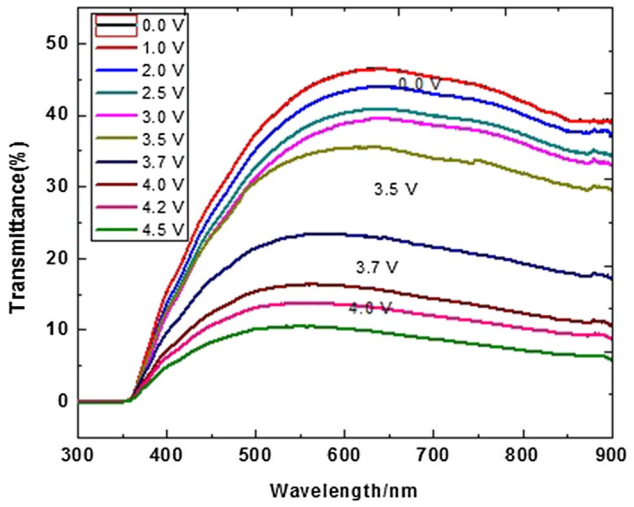

Fig. 9 Transmittance spectra of the electrochromic devices fabricated with optimized PAN nanofiber membrane gel polymer electrolyte at different electrochemical statuses under different applied voltages

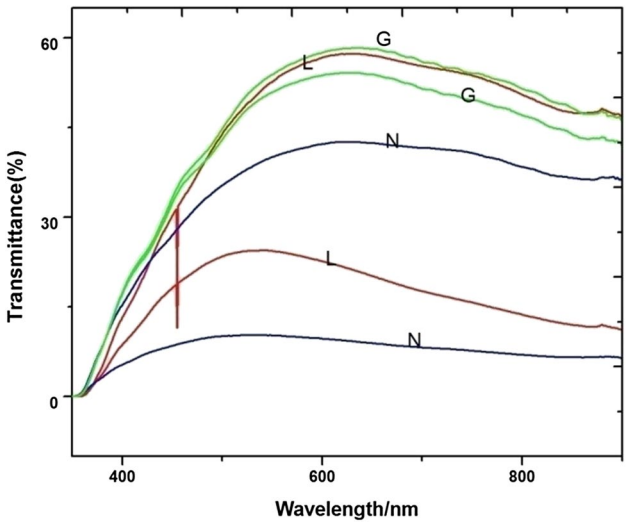

Fig. 10 Transmittance variation of ECDs at colored and bleached state with PAN nanofiber membrane gel electrolyte (N) with optimized thickness, liquid electrolyte (L), and conventional PAN-based gel electrolyte (G)

where $T_b(\lambda)$ is the maximum transmittance at the colorless state and $T_c(\lambda)$ is the transmittance at the colored state at the same wavelength.

Figure 9 shows the transmittance spectra of the electrochromic devices fabricated with PAN nanofiber membrane gel polymer electrolyte at different electrochemical statuses under different applied voltages (0–4.2 V) in the wavelength range from 350 to 900 nm.

Performance was checked for the three types of the ECDs fabricated (a) with conventional liquid electrolyte comprising 1 M $LiClO_4$ in PC (L), (b) with PAN-based nanofiber membrane gel electrolyte with optimized membrane thickness (N), and (c) conventional PAN gel electrolyte with the same composition (G). Figure 10 shows the comparison of transmittance variation of the devices at their fully colored state and bleached state under the same applied voltage comprising three different types of electrolytes mentioned above.

The summary of the performances of ECDs measured for the three different types of electrolytes is shown in Table 2. It can be seen that the transmittance difference ΔT between the colored and bleached states of the EC made with the PAN-based nanofiber gel electrolyte is about 93% of that obtained for the liquid electrolyte–based EC.

As the nanofiber membrane has a more porous network structure as shown by the SEM images, it is possible to prepare a "nanofiber membrane gel" electrolyte by soaking the nanofiber mat in the liquid electrolyte solution. Nanostruturally, this is different to the "conventional gel" electrolyte, prepared simply by dissolving the polymer in the electrolyte solution. Therefore, the ionic mobility in the nanofiber gel electrolyte is close to the ionic mobility in the corresponding liquid electrolyte. On the other hand, the conventional gel electrolyte, prepared by dissolving the polymer in the liquid electrolyte, restricts the Li ion mobility in the electrolyte due to its viscous nature. Also, the low viscosity of the liquid electrolyte and nanofiber membrane gel electrolyte provides an ionic environment that facilitates ionic mobility while the conventional gel electrolyte having a relatively higher viscosity provides low ionic mobility. Therefore, compared to the liquid and the nanofiber membrane gel electrolytes, the conventional PAN-based gel electrolyte exhibits poor ionic mobility for Li ions that can reach the electrochromic TiO_2 electrode. This could be the reason for improved ECD performance when using nanofiber membrane gel lectrolyte compared to the conventional gel electrolyte.

Stability and coloration time of the PAN nanofiber–based electrochomic device

Figure 11a shows the cyclic voltammograms (CV) obtained for the first, 250th, and 500th cycles. According to the figure, oxidation and reduction peaks can be identified due to the existence of lithium in the nanofiber membrane electrolyte. These peaks represent chemical reactions that take place at

Table 2 Transmittance variation of the ECDs with liquid electrolyte, nanofiber membrane electrolyte, and gel electrolyte

Type of the electrolyte	Transmittance at 4.2 V	Transmittance at 0 V	ΔT
Liquid 1 M $LiClO_4$ in PC	21.40	57.35	35.95
PAN nanofiber + 1 M $LiClO_4$ in PC	13.09	46.49	33.40
PAN gel	54.11	58.33	4.22

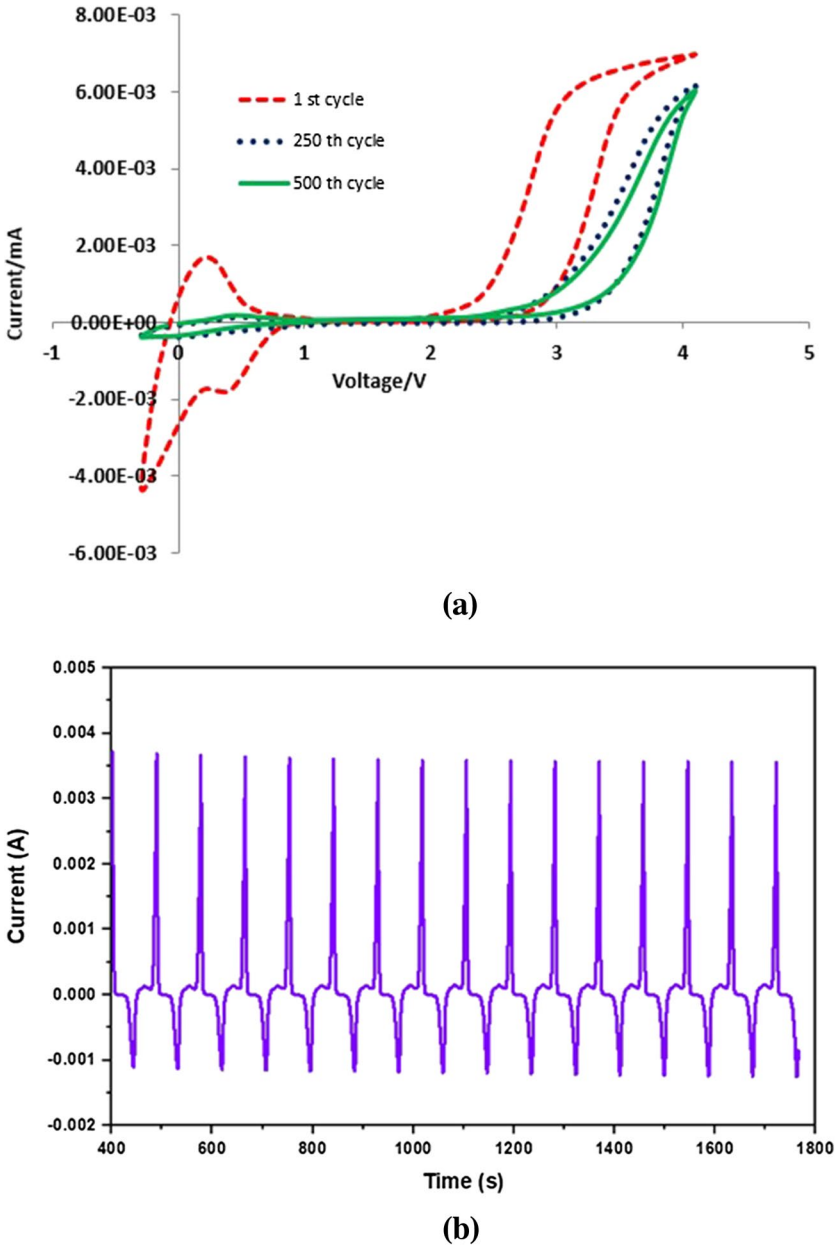

Fig. 11 **a** Cyclic voltammograms for an ECD with the configuration FTO/TiO 2/nanofiber membrane electrolyte/SnO_2/FTO for the 1st, 250th, and 500th cycles. Scan rate 100 mVs^{-1}. **b** Variation of current with time for different cycle

the surface of the FTO. The feature of the voltammogram changes within the first few cycles, but the shape of the cyclic voltammogram does not change sharply by cycling up to 500 cycles. The current density at the cathodic peak which corresponds to the bleaching process gradually increased up to the 250th cycle and then remained constant while the current density for the coloration process which characterizes the charge intercalation into TiO_2 decreased within the first few cycles. However, there is no significant change in either the shape of CV or current densities beyond the 250th cycle, suggesting that the device with the configuration of FTO glass/TiO_2/nanofiber membrane electrolyte/SnO_2/FTO glass has moderately high stability. This is confirmed by the current time graph obtained for the CV (Fig. 11b). Percent change in current density was calculated (Eq. 2).

$$Percent\ change\ in\ current\ density = \frac{Change\ of\ current\ density\ within\ 30\ minutes}{Initial\ current\ density} \times 100\% \quad (2)$$

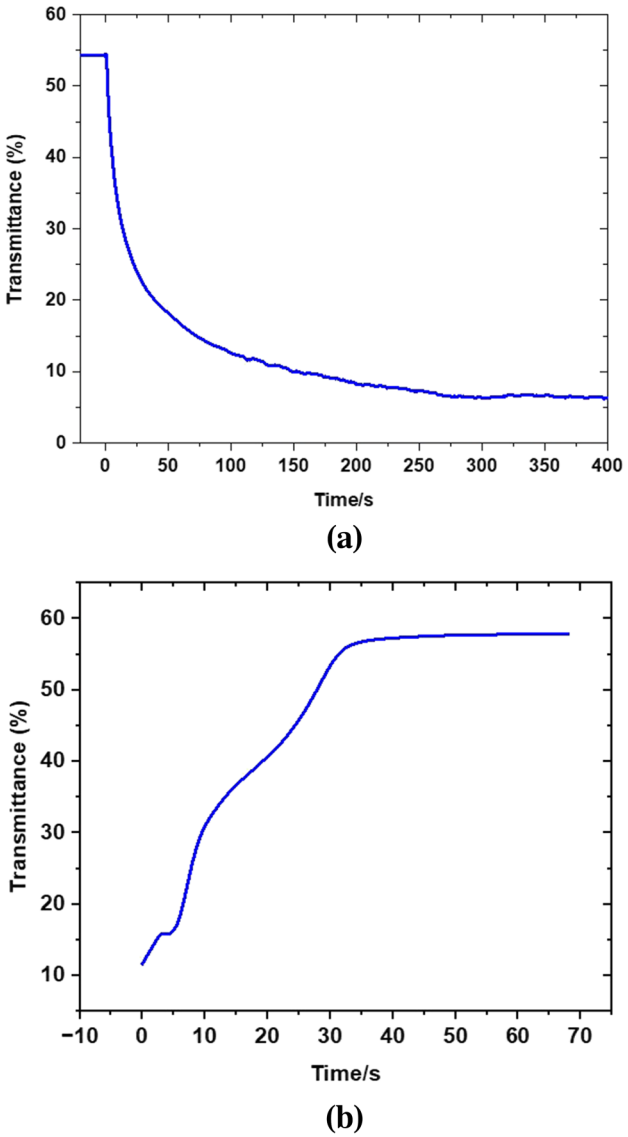

Fig. 12 **a** Time for coloration of the ECD. **b** Time for bleaching of the ECD

According to the above equation, percent change in current density during the first 30 min is 12.5%. However, for the second 30 min up to 1 h totally, the percent change of current density remains unchanged.

The coloration time t_c (the time taken to reduce the light transmission through the ECD from 90 to 10% in the coloration process) and decoloring time or bleaching time t_b (the time taken to intense the light transmittance through the ECD from 10 to 90% in the decoloring process) were measured [38]. Under this definition, coloration and decoloration time for the ECDs of configuration FTO glass/TiO_2/nanofiber membrane electrolyte/SnO_2/FTO glass were around 75 s and 40 s respectively (Fig. 12a and b). Coloration time of the nanofiber-based ECD was measured and relativle high coloration time of 75 s was observed which is compatible for architectural applications.

Table 3 represents the electrochromic performance of the ECDs fabricated with different polymer nanofibers. Application of PAN nanofiber for TiO_2-based electrochromic devices has not been reported so far. In comparison with the previously published data, ECDs fabricated in this study shows comparative chromatic contrast (ΔT).

Conclusion

The electrospinning method was used to successfully prepare a novel PAN-based nanofiber membrane gel electrolyte. The morphology of a PAN-based nanofiber membrane gel electrolyte was studied using SEM images at an optimized electrospinning time of 10 min. ECDs fabricated with nanofiber membrane gel electrolyte together with low-cost TiO_2 and SnO_2 metal oxides as the electrochromic material and counter electrode respectively showed desirable electrochromic properties. A reversible color change between dark blue and colorless status was observed when an appropriate voltage was applied to the electrochromic device. Optimized nanofiber membrane gel electrolyte showed optical

Table 3 Comparison of electrochromic performance

Polymer used to prepare nanofiber	EC material	Δ*T*	Coloration time/s	Bleaching time/s	Reference
PAN	TiO_2	33.4	75 s	40	This paper
Poly(ε-caprolactone)	poly(3,4-ethylene-dioxythiophene) PEDOT		40.5	16.2	[39]
Polypyrrole	WO_3	47.41	5.74	0.89	[34]
Poly(vinylidene fluoride-co-trifluoroethylene) (PVDF-TrFE)	Dihexyl viologen-hexafluorophosphate	39	20	8	[40]
Polypyrrole/PMMA	WO_3/PEDOT	40.42	0.31	6.53	[41]
PANI	Cr	54.1	0.085	0.062	[42]
PANI	SnO_2/Sb/TiO_2	38.5	1.2	1.0	[43]

modulation of 33.40% between its colored and bleached states whereas liquid electrolyte showed comparable value of 35.95% for an identical cell. This demonstrates that the incorporation of quasi-solid-state PAN nanofiber membrane electrolytes renders comparable performance with liquid-state electrolytes in ECDs.

Author contribution H.N.M. Sarangika, the Corresponding author and the first author did the experimental part under the supervision of Prof. M.A.K.L. Dissanayake and Prof. G.K.R. Senadeera. H.N.M. Sarangika wrote the manuscript and Prof. M.A.K.L. Dissanayake and Prof. G.K.R. Senadeera reviewed the manuscript.

Data availability Not applicable.

Declarations

Ethical approval This article does not involve human or biological research and has no moral or ethical issues.

Competing interests The authors declare no competing interests.

References

1. Thakur VK, Ding G, Ma J et al (2012) Hybrid materials and polymer electrolytes for electrochromic device applications. Adv Mater 24:4071–4096. https://doi.org/10.1002/adma.201200213
2. Shah KW, Wang S-X, Soo DXY, Xu J (2019) Viologen-based electrochromic materials: from small molecules, polymers and composites to their applications. Polymers (Basel) 11:1839. https://doi.org/10.3390/polym11111839
3. Silva MM, Barbosa PC, Rodrigues LC et al (2010) Gelatin in electrochromic devices. Opt Mater (Amst) 32:719–722. https://doi.org/10.1016/j.optmat.2009.08.013
4. Fernandes M, Leones R, Costa AMS et al (2015) Electrochromic devices incorporating biohybrid electrolytes doped with a lithium salt, an ionic liquid or a mixture of both. Electrochim Acta 161:226–235. https://doi.org/10.1016/j.electacta.2015.02.036
5. Rosseinsky DR, Mortimer RJ (2001) Electrochromic systems and the prospects for devices. Adv Mater 13:783–793. https://doi.org/10.1002/1521-4095(200106)13:11%3c783::AID-ADMA783%3e3.0.CO;2-D
6. Huang B, Zhang Y, Que M et al (2017) A facile in situ approach to ion gel based polymer electrolytes for flexible lithium batteries. RSC Adv 7:54391–54398. https://doi.org/10.1039/C7RA10268B
7. Sarangika HNM, Dissanayake MAKL, Senadeera GKR, Karunarathne WGMD (2020) Low cost quasi solid state electrochromic devices based on F-doped tin oxide and TiO_2. Mater Today Proc 23:100–104. https://doi.org/10.1016/j.matpr.2019.07.585
8. Barbosa PC, Rodrigues LC, Silva MM et al (2010) Solid-state electrochromic devices using pTMC/PEO blends as polymer electrolytes. Electrochim Acta 55:1495–1502. https://doi.org/10.1016/j.electacta.2009.03.031
9. Kim YM, Seo DG, Oh H, Moon HC (2019) A facile random copolymer strategy to achieve highly conductive polymer gel electrolytes for electrochemical applications. J Mater Chem C 7:161–169. https://doi.org/10.1039/C8TC05092A
10. Zhang F, Dong G, Liu J et al (2017) Polyvinyl butyral-based gel polymer electrolyte films for solid-state laminated electrochromic devices. Ionics (Kiel) 23:1879–1888. https://doi.org/10.1007/s11581-017-1996-y
11. Xu X, Shirakashi Y, Ishibashi J et al (2012) Mechanism of surface roughness development in melt spinning of blend fibers for artificial hair. Text Res J 82:1382–1389. https://doi.org/10.1177/0040517512441993
12. Lambrecht J, Saragi TPI, Salbeck J (2011) Self-assembled organic micro-/nanowires from an air stable n-semiconducting perylenediimide derivative as building blocks for organic electronic devices. J Mater Chem 21:18266. https://doi.org/10.1039/c1jm13998c
13. Tomioka K, Motohisa J, Hara S, Fukui T (2008) Control of InAs nanowire growth directions on Si. Nano Lett 8:3475–3480. https://doi.org/10.1021/nl802398j
14. Tanaka M (2016) Development of ion conductive nanofibers for polymer electrolyte fuel cells. Polym J 48:51–58. https://doi.org/10.1038/pj.2015.76
15. Wang J, Zhang L, Yu L et al (2014) A bi-functional device for self-powered electrochromic window and self-rechargeable transparent battery applications. Nat Commun 5:4921. https://doi.org/10.1038/ncomms5921
16. Aqueel Ahmed AT, Hou B, Inamdar AI et al (2019) Morphology engineering of self-assembled nanostructured $CuCo_2O_4$ anodes for lithium-ıon batteries. Energy Technol 7. https://doi.org/10.1002/ente.201900295
17. Li C, Qin B, Zhang Y et al (2019) Single-ıon conducting electrolyte based on electrospun nanofibers for high-performance lithium batteries. Adv Energy Mater 9. https://doi.org/10.1002/aenm.201803422
18. Li D, Xia Y (2004) Electrospinning of nanofibers: reinventing the wheel? Adv Mater 16:1151–1170. https://doi.org/10.1002/adma.200400719
19. Teo WE, Ramakrishna S (2006) A review on electrospinning design and nanofibre assemblies. Nanotechnology 17:R89–R106. https://doi.org/10.1088/0957-4484/17/14/R01
20. Arai T, Kawakami H (2012) Ultrafine electrospun nanofiber created from cross-linked polyimide solution. Polymer (Guildf) 53:2217–2222. https://doi.org/10.1016/j.polymer.2012.03.059
21. Fukushima S, Karube Y, Kawakami H (2010) Preparation of ultrafine uniform electrospun polyimide nanofiber. Polym J 42:514–518. https://doi.org/10.1038/pj.2010.33
22. Reneker DH, Yarin AL (2008) Electrospinning jets and polymer nanofibers. Polymer (Guildf) 49:2387–2425. https://doi.org/10.1016/j.polymer.2008.02.002
23. Wu W-N, Yu H-F, Yeh M-H, Ho K-C (2020) Incorporating electrospun nanofibers of TEMPO-grafted PVDF-HFP polymer matrix in viologen-based electrochromic devices. Sol Energy Mater Sol Cells 208:110375. https://doi.org/10.1016/j.solmat.2019.110375
24. Mailley D, Hébraud A, Schlatter G (2021) A review on the ımpact of humidity during electrospinning: from the nanofiber structure engineering to the applications. Macromol Mater Eng 306. https://doi.org/10.1002/mame.202100115
25. Yang P, Sun P, Chai Z et al (2014) Large-scale fabrication of pseudocapacitive glass windows that combine electrochromism and energy storage. Angew Chemie 126:12129–12133. https://doi.org/10.1002/ange.201407365
26. Zhou D, Shi F, Xie D et al (2016) Bi-functional Mo-doped WO_3 nanowire array electrochromism-plus electrochemical energy storage. J Colloid Interface Sci 465:112–120. https://doi.org/10.1016/j.jcis.2015.11.068
27. Cai G, Wang J, Lee PS (2016) Next-generation multifunctional electrochromic devices. Acc Chem Res 49:1469–1476. https://doi.org/10.1021/acs.accounts.6b00183
28. Akkurt N, Pat S, Mohammadigharehbagh R et al (2020) Investigation of TiO_2 thin films as a cathodic material for electrochromic

display devices. J Mater Sci Mater Electron 31:9568–9578. https://doi.org/10.1007/s10854-020-03499-0
29. Dissanayake MAKL, Jaseetharan T, Senadeera GKR, Kumari JMKW (2020) Efficiency enhancement in PbS/CdS quantum dot-sensitized solar cells by plasmonic Ag nanoparticles. J Solid State Electrochem 24:283–292. https://doi.org/10.1007/s10008-019-04420-4
30. Senadeera GKR, Nakamura K, Kitamura T et al (2003) Fabrication of highly efficient polythiophene-sensitized metal oxide photovoltaic cells. Appl Phys Lett 83:5470–5472. https://doi.org/10.1063/1.1633673
31. Senadeera GKR, Sandamali WI, Kumari JMKW et al (2022) Morphological and structural study on low cost SnO_2 counter electrode and its applications in quantum dot sensitized solar cells with polysulfide electrolyte. Mater Sci Eng B 286:116075. https://doi.org/10.1016/j.mseb.2022.116075
32. Dissanayake MAKL, Divarathne HKDWMNR, Thotawatthage CA et al (2014) Dye-sensitized solar cells based on electrospun polyacrylonitrile (PAN) nanofibre membrane gel electrolyte. Electrochim Acta 130:76–81. https://doi.org/10.1016/j.electacta.2014.02.122
33. Dissanayake MAKL, Thotawatthage CA, Senadeera GKR et al (2012) Efficiency enhancement by mixed cation effect in dye-sensitized solar cells with PAN based gel polymer electrolyte. J Photochem Photobiol A Chem 246:29–35. https://doi.org/10.1016/j.jphotochem.2012.06.023
34. Dulgerbaki C, Maslakci NN, Komur AI, Oksuz AU (2018) Electrochromic strategy for tungsten oxide/polypyrrole hybrid nanofiber materials. Eur Polym J 107:173–180. https://doi.org/10.1016/j.eurpolymj.2018.07.050
35. Priya ARS, Subramania A, Jung Y-S, Kim K-J (2008) High-performance quasi-solid-state dye-sensitized solar cell based on an electrospun PVdF−HFP membrane electrolyte. Langmuir 24:9816–9819. https://doi.org/10.1021/la801375s
36. Choi Y-J, Kim D-W (2011) Photovoltaic performance of dye-sensitized solar cells assembled with hybrid composite membrane based on polypropylene non-woven matrix. Bull Korean Chem Soc 32:605–608. https://doi.org/10.5012/bkcs.2011.32.2.605
37. Eren O, Ucar N, Onen A et al (2016) Synergistic effect of polyaniline, nanosilver, and carbon nanotube mixtures on the structure and properties of polyacrylonitrile composite nanofiber. J Compos Mater 50:2073–2086. https://doi.org/10.1177/0021998315601891
38. Gunathilaka HMBI, Seneviratne VA, Sarangika HNM (2023) Polymer-free gel electrolyte and its application in TiO_2-based electrochromic devices. J Appl Electrochem 53:2185–2196. https://doi.org/10.1007/s10800-023-01912-0
39. Liu X, Li K, Hou C et al (2019) Poly-ε-caprolactone nanofibrous mats as electrolyte host for tailorable flexible electrochromic devices. Mater Sci Eng B 241:36–41. https://doi.org/10.1016/j.mseb.2019.02.001
40. Choi JH, Pande GK, Lee YR, Park JS (2020) Electrospun ion gel nanofibers for high-performance electrochromic devices with outstanding electrochromic switching and long-term stability. Polymer (Guildf) 194:122402. https://doi.org/10.1016/j.polymer.2020.122402
41. Dulgerbaki C, Komur AI, Nohut Maslakci N et al (2017) Synergistic tungsten oxide/organic framework hybrid nanofibers for electrochromic device application. Opt Mater (Amst) 70:171–179. https://doi.org/10.1016/j.optmat.2017.05.024
42. Erro EM, Baruzzi AM, Iglesias RA (2014) Fast electrochromic response of ultraporous polyaniline nanofibers. Polymer (Guildf) 55:2440–2444. https://doi.org/10.1016/j.polymer.2014.03.050
43. Zhang S, Chen S, Yang F et al (2019) High-performance electrochromic device based on novel polyaniline nanofibers wrapped antimony-doped tin oxide/TiO_2 nanorods. Org Electron 65:341–348. https://doi.org/10.1016/j.orgel.2018.11.036